LA-UR 93-0165

LA-UR--93-165

DE93 007344

Los Alamos National Laboratory is operated by the University of California for the United States Department of Energy under contract W-7405-ENG-36.



TITLE WEAKLY NONLINEAR DYNAMICS OF NEAR-CJ DETONATION WAVES

AUTHOR(S): John B. Bdzil, M-7, P950

Rupert Klein
Institut Fur Technische Mechanik, RWTH
Templergraben 64, 5100 Aachen, Germany

SUBMITTED TO Proceedings of ICASE Symposium on Hypersonic Propulsion, October 1992 ICASE/NASA, Langely Virginia

## DISCLAIMER





Los Alamos National Laboratory
Los Alamos, New Mexico 87545

# WEAKLY NONLINEAR DYNAMICS OF NEAR-CJ DETONATION WAVES

*John B. Bdzil* & Rupert Klein***

* M-7 - MS P952, Los Alamos National Laboratory
Los Alamos, New Mexico, 87545

** Institut für Technische Mechanik, RWTH
Templergraben 64, 5100 Aachen, Germany

## ABSTRACT

The renewed interest in safety issues for large scale industrial devices and in high speed combustion has driven recent intense efforts to gain a deeper theoretical understanding of detonation wave dynamics. Linear stability analyses, weakly nonlinear bifurcation calculations as well as full scale multi-dimensional direct numerical simulations have been pursued for a standard model problem based on the reactive Euler equations for an ideal gas with constant specific heat capacities and simplified chemical reaction models. Most of these studies are concerned with overdriven detonations. This is true despite the fact that the majority of all detonations observed in nature are running at speeds close to the Chapman-Jouguet (CJ) limit value. By focusing on overdriven waves one removes an array of difficulties from the analysis that is associated with the sonic flow conditions in the wake of a CJ-detonation. In particular, the proper formulation of downstream boundary conditions in the CJ-case is a yet unsolved analytical problem.

A proper treatment of perturbations in the back of a Chapman-Jouguet detonation has to account for two distinct weakly nonlinear effects in the forward acoustic wave component. The first is a nonlinear interaction of highly temperature sensitive chemistry with the forward acoustic wave component in a transonic boundary layer near the end of the reaction zone. The second is a cumulative three-wave-resonance in the sense of Majda et al. which is active in the near-sonic

burnt gas flow and which is essentially independent of the details of the chemical model. In this work, we consider detonations in mixtures with moderate state sensitivity of the chemical reactions (no large activation energy). Then, the acoustic perturbations do not influence the chemistry at the order considered and we may concentrate on the second effect; the three-wave resonance.

## 1. Introduction

The theory of detonation waves has recently regained much attention in connection with safety issues in large scale industrial devices, (Shepherd (1985), Breitung (1991)), or the storage of condensed phase explosives and also in connection with the problem of efficient controlled high Mach number combustion in high speed airplane engines (Shepherd (1992)). The goal is to improve the understanding of detonation wave stability and to design efficient numerical tools for direct simulations based on detailed physical insight. In both these problem areas, detonation stability (Erpenbeck (1962, 63, 64), Lee and Stewart (1991)) and direct numerical simulations (Oran and Boris (1987), Fujiwara and Reddy (1989), Schoeffel (1989), Bourlioux (1991) and Bourlioux and Majda (1992)), the formulation of downstream, i.e., burnt gas side, boundary conditions is crucial for an accurate representation of the phenomena. The standard approach is to suppress the forward acoustic mode at the downstream boundary so as to mimic a combustion wave that is evolving without any perturbations being imposed from outside, (Lee and Stewart (1990)). We will refer to this approach below as the "standard radiation condition". Here and below the expression "forward" labels acoustic perturbations facing in the direction of propagation of the detonation in the laboratory frame. In the present setting, for a wave running from right to left, this means that forward acoustic characteristics travel at speed $(\partial z/\partial t)^- = u - c$, where $u$ and $c$ are the local flow velocity and the speed of sound, respectively.

The physically most interesting class of detonations is that of near-Chapman-Jouguet(CJ) waves, for which an acoustic decoupling between the detonation wave structure and the burnt gas flow occurs. In section 2 we briefly summarize for convenience the ZND detonation theory following Fickett and Davis (1979). In section 3 we show that in the CJ-regime there is a generation of nonzero forward acoustic perturbations in the burnt gases through weakly

nonlinear three-wave resonance of the type first discussed in a different context by Majda and Rosales (1984), Majda et al. (1988). Thus, even if no forward-acoustic perturbations are present at some initial time in the burnt gas region, they are generated automatically through interactions of backward traveling perturbations that emerge from the detonation structure as time evolves. This observation obviously questions the standard radiation condition, since the latter is equivalent to suppressing the forward acoustic mode in the farfield. Our goal in this paper is to resolve this apparent contradiction using methods of asymptotic analysis.

To see what is involved, one needs to compare two characteristic length scales. One is the distance behind the lead shock of the detonation where numerical boundary conditions are imposed. The second is the length scale for the three-wave resonance phenomena mentioned above. Let $\epsilon$ be the small perturbation amplitude used as an expansion parameter. (Later on we consider $\epsilon$ to be the growth rate of the most unstable Eigenmode of a marginally stable detonation.) Figure 1 shows a sketch of the spatial distribution of a representative reaction progress variable, $(1-\lambda)$, in a ZND-detonation, where the unburnt gas is approaching from the left and the lead shock is located at $x = 0$. At the lead shock there is pure unburnt gas so that $(1-\lambda) = 1$, and as $x \to \infty$ and $(1-\lambda) \to 0$, we approach the burnt gas region.

Numerical linear stability codes, (Lee and Stewart (1990)), resolve a region $0 \leq x < x_{1/N}$, where $x_{1/N}$ is the location where $(1-\lambda) = 1/N$ and $N$ is the number of grid points in the discretized linear perturbation equations. Notice that

$$x_{1/N} = O(1) \qquad \text{as} \qquad \epsilon \to 0\,, \tag{1.1}$$

i.e., in terms of the perturbation amplitude the downstream boundary condition is imposed at a finite distance. In contrast , the three-wave resonance occurs at distances

$$x = O(1/\epsilon^2). \tag{1.2}$$

The key question is what will become of the forward acoustic perturbations generated at these large distances as they move up to the detonation structure and finally arrive at the position $x_{1/N}$ where they would influence the numerical downstream boundary conditions.

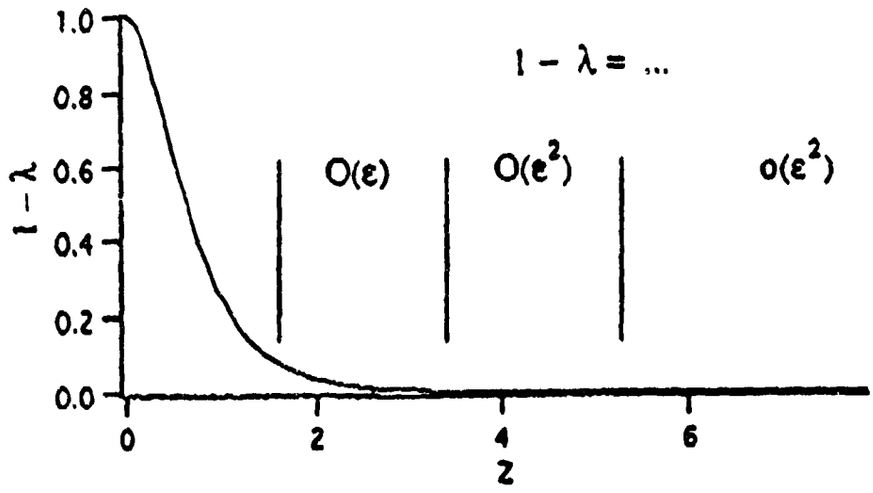


Fig. 1: Spatial distribution of the reaction progress variable in a CJ-ZND detonation and identification of several asymptotic layers.

One may answer this question by using the method of matched asymptotic expansions: Simplified asymptotic descriptions of the solution in four distinct regions have to be matched. There is a main reaction layer where $(1-\lambda) = O(1)$, an intermediate transonic layer where $(1-\lambda) = O(\epsilon)$, a burnout layer where $(1-\lambda) = O(\epsilon^2)$, and the burnt gas region where $(1-\lambda) \ll \epsilon^2$. The acoustic resonances are dominant in the latter two regions and the present paper focuses on their analysis. The principal facts relevant for the formulation of downstream boundary conditions are readily demonstrated in this paper through a combination of formal asymptotic arguments and numerical solutions of the burnout layer equations. We leave detailed numerical studies of the burnt gas resonance effects, the tedious calculations for the transonic region and the final matching to the main reaction layer for a later publication, (Bdzil and Klein (1993)).

Section 3 of this paper discusses the burnt gas region, $z = O(1/\epsilon^2)$, where the chemical activity is negligible. We summarize the equations for weakly nonlinear three-wave resonance and define a model problem suited to exhibit the generation of forward acoustic perturbations. It turns out, however, that on the time scales considered the

perturbations near the end of the reaction zone, e.g., at $z_{1/N}$ from (1.1), are related directly to the asymptotic solutions in the burnout layer. There the chemical source terms appear at order $O(\epsilon^2)$ and modify the acoustic resonance equations. Thus we concentrate on this region in section 4 and develop formal solutions based on the method of characteristics as well as numerical solutions including shock discontinuities. The main influence of the chemical source terms is to continously accelerate and amplify the forward acoustic perturbations and to establish a reaction tail that matches into the unperturbed CJ-ZND structure. Both the formal characteristic solution and the numerical solutions show the expected behavior – an energy transfer from the backward acoustic mode into forward acoustic perturbations. Both approaches predict that the effects of weakly nonlinear acoustic resonance decay as the forward characteristics move upstream into the transonic region.

This tendency is approved in Bdzil and Klein (1993) where we show that the resonance effects are down to order $O(\epsilon^2)$ at finite distances where numerical boundary conditions are imposed and we conclude that:

> The standard radiation condition imposed at some finite distance $z_{1/N}$ behind the lead shock is valid even for Chapman-Jouguet detonations.

Our approach is the first to use rational asymptotic methods to resolve the boundary difficulties that arise in the stability problem for plane CJ-detonation. Our success at resolving the boundary condition difficulties that have been a part of linear stability analyses of detonation since Erpenbeck (1962), (1963), (1964), suggests this same approach for other problems; notably the confusing "square wave" detonation stability problem and the problem of oblique detonation stability in the CJ-like critical regime.

## 2. The ZND Detonation Model

We analyse the dynamics of fast combustion waves in the framework of a standard model for gaseous detonations. A plane ZND-detonation (see Fickett and Davis (1979)) consists of a leading inviscid shock wave and a subsequent zone of chemical activity. The lead shock heats up and compresses the gas so that exothermal chemical reactions are turned on. The chemical energy is converted into thermal and kinetic energy thereby overcoming all or part of the dissipation in the lead shock. For a given combustible there is a continous family of ZND detonations parametrized by the detonation speed, $D$. The so-called Chapman-Jouguet detonations are those with the smallest possible speed $D = D_{CJ}$. The main characteristic feature of a CJ-detonation needed in our analysis is the fact that forward acoustic perturbations in the burnt gases travel at exactly the same speed as the detonation itself. In other words, the burnt gases move away from the detonation structure at (their own) sonic speed. Figure 2 shows a space-time diagram for a CJ-detonation traveling from right to left with the unburnt gas at rest in the laboratory frame of reference. We display the path of the leading shock, indicate the reaction zone and exhibit a family of forward acoustic characteristics.

The ZND detonation structure is described by traveling wave solutions of the reactive Euler equations

$$\underline{U}_t + \underline{\underline{A}}(\underline{U})\underline{U}_x = \underline{G}(\underline{U}), \tag{2.1}$$

where $(x,t)$ are laboratory coordinates and

$$\underline{U} = (v, \bar{u}, p, \lambda)^t, \tag{2.2}$$

with $v$ the specific volume, $\bar{u}$ the flow velocity in the laboratory frame, $p$ the pressure and $\lambda$ a reaction progress variable satisfying $\lambda = 0$ in the unburnt and $\lambda = 1$ in the burnt gas. Furthermore

$$\underline{\underline{A}}(\underline{U}) = \begin{pmatrix} \bar{u} & -v & 0 & 0 \\ 0 & \bar{u} & v/\gamma & 0 \\ 0 & \gamma p & \bar{u} & 0 \\ 0 & 0 & 0 & \bar{u} \end{pmatrix} \tag{2.3}$$

and

$$\underline{G}(\underline{U}) = (0, 0, \frac{\gamma - 1}{v} Qr, r)^t, \tag{2.4}$$

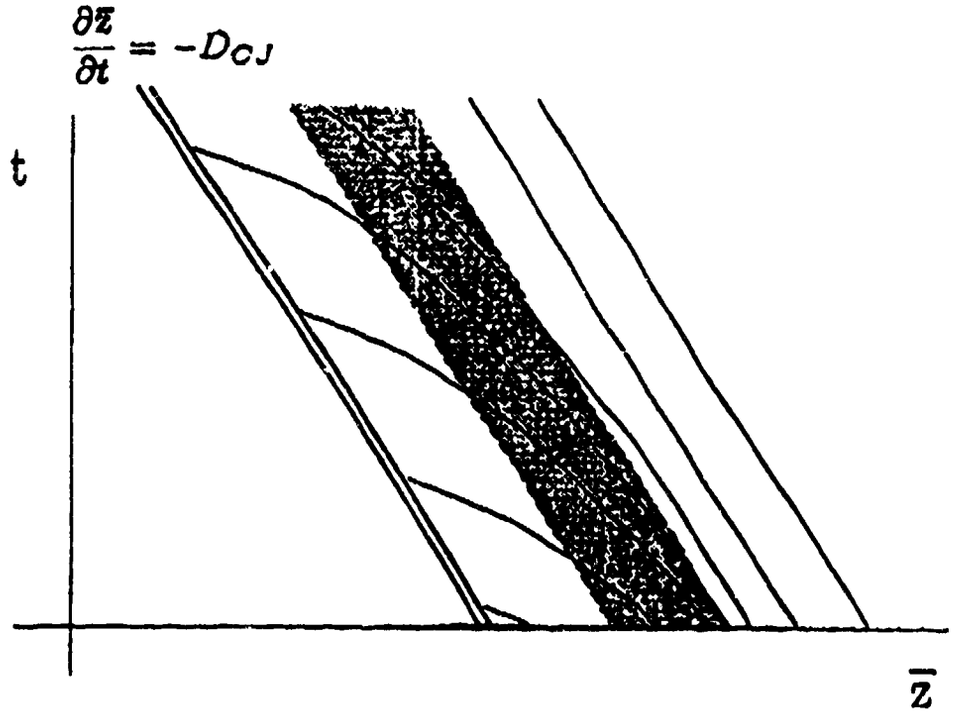


Fig. 2: Wave diagram for forward acoustic perturbations in the wake of a Chapman-Jouguet detonation travelling from right to left in a laboratory frame.

where $\gamma$ is the isentropic exponent, $Q$ a dimensionless chemical heat of reaction and

$$r = K(p, v)(1 - \lambda) \tag{2.5}$$

the reactionrate. For simplicity in the derivations we have assumed an ideal gas with constant specific heats so that $\gamma$ = const. The above equations are supplemented by shock jump conditions at

$$z = \bar{z} + D_{CJ}\, t = 0 \tag{2.6}$$

(see e.g., Fickett and Davis (1979), Lee and Stewart (1990)) and one seeks traveling wave solutions so that $\underline{U} = \underline{U}^*(z)$ where $z$ is a front attached coordinate according to (2.6).

The equations are nondimensionalized using the reference quantities

| | | | |
|---|---|---|---|
| specific volume | : | $v_{sh}$ | |
| pressure | : | $P_{sh}$ | |
| velocity | : | $c_{sh} = \sqrt{\gamma P_{sh} v_{sh}}$ | (2.7) |
| length | : | half-reaction length $l_{1/2}$ | |
| time | : | $l_{1/2}/c_{sh}$ . | |

The half reaction length is defined as the distance behind the lead shock where $\lambda = 1/2$ and the subscript "sh" denotes the post-shock (von Neumann) conditions.

With this nondimensional representation, the exact solution for the Chapman-Jouguet - ZND detonation structure can be written in terms of the reaction progress variable, $\lambda = \lambda^*(z)$, as, (Lee and Stewart (1990)),

$$\begin{aligned} p^* &= a^* + (1 - a^*)(1 - \lambda^*)^{1/2}, \\ v^* &= \tfrac{1-p^*}{\gamma M_{sh}^2} + 1, \\ u^* &:= \bar{u}^* + D_{CJ} = v^* M_{sh}, \end{aligned} \tag{2.8}$$

where $M_{sh} = D_{CJ}/c_{sh}$ and

$$a^* = \frac{\gamma M_{sh}^2 + 1}{\gamma + 1}. \tag{2.9}$$

Equations (2.8) express the detonation structure solely in terms of the reaction progress variable $\lambda^* = \lambda^*(z)$. The spatial distribution of all quantities follows from solving the fourth equation in (2.1):

$$u^* \lambda_z^* = r(p^*, v^*, \lambda^*), \tag{2.10}$$

with $u^*$, $v^*$, $p^*$, $r^*$ from (2.8), (2.5) as functions of $\lambda^*$. We notice, in particular, that $u^* - \sqrt{p^* v^*} = 0$ at $(\lambda^* = 1)$, i.e. that the burnt gas flow is sonic.

## 3. Weakly Nonlinear Resonant Acoustics in the Farfield

### 3.1 The burnt gas region

Consider a marginally stable CJ-detonation that oscillates with a small slowly varying amplitude in the frame of reference moving with the unperturbed wave as sketched in Fig. 3. Under CJ-conditions, one has $|u_{CJ}| = c_{CJ}$, such that

$$(u - c)_{CJ} = 0\,, \quad u_{CJ} + c_{CJ} = 2u_{CJ} = 2c_{CJ}\,. \tag{3.1}$$

Entropy perturbations generated by the oscillations of the detonation speed and by perturbations of the reaction process travel backwards into the burnt gases at speed $(\partial z/\partial t) = u_{CJ}$, while backward acoustic perturbations travel at $(\partial z/\partial t) = u_{CJ} + c_{CJ} = 2u_{CJ}$. Since these perturbations are generated in phase within the detonation structure, their associated spatial wave lengths in the burnt gas region differ by exactly a factor of two. From the theory of weakly nonlinear resonant acoustics by Majda and Rosales (1984) one knows that this is the condition for cumulative resonant generation of forward acoustic perturbations. These are of the same order of magnitude as the backward traveling perturbations and apparently cannot be suppressed. To be more specific we propose the following model problem that allows one to give a quantitative description of the resonance and of its effects near the end of the detonation reaction zone.

A CJ-detonation with a marginally stable structure is perturbed at time $t = 0$. In a suitable frame of reference the wave will typically start to oscillate around its unperturbed position at a frequency given by the imaginary part, $\alpha_i$, of the Eigenvalue associated with the most unstable eigenmode. The perturbations of the detonation speed and of the reaction process generate entropy and backward acoustic perturbations. These leave the reaction zone and radiate into the burnt gases. We are interested in the long time behavior of the radiation field in the back of the wave. We assume the entropy and backward acoustic perturbations to be given in the form of sinusoidal oscillations at the edge of the reaction zone; more precisely at some

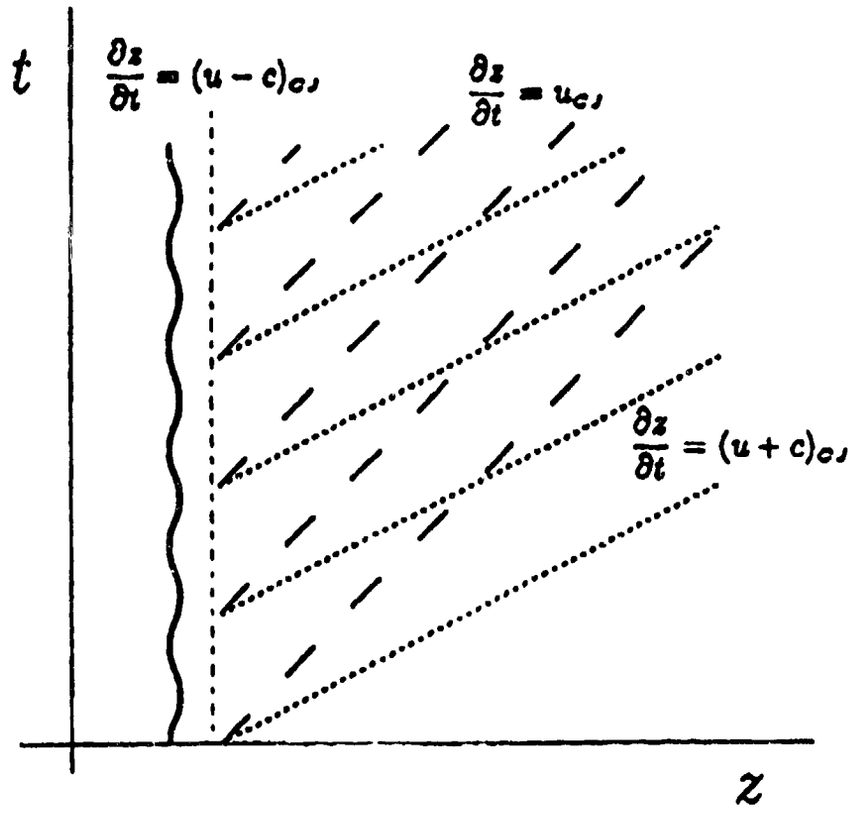


Fig. 3: Characteristics in the burnt gas behind a marginally stable CJ-detonation.

location $z = z_3$ where $(1 - \lambda^*) = \epsilon^3$ so that for $z \sim z_3$ according to (2.5) the reaction source terms are negligible up to and including the second order in $\epsilon$. Then we have to solve the following initial-boundary value problem up to first order in $\epsilon$ for the inert Euler equations,

$$\underline{U}_t + \underline{\underline{A}}(\underline{U})\underline{U}_z = 0 \quad (z > z_3\,,\, t \geq 0)\,, \tag{3.2}$$

with initial conditions

$$\underline{U}(z,0) = \underline{U}_{CJ} \quad (z > z_3) \tag{3.3}$$

and boundary conditions at $z = z_3$ for the entropy and backward acoustic modes given by

$$\begin{aligned} \underline{l}^0 \cdot \underline{U}(z_3,t;\epsilon) &= \underline{l}^0 \cdot \underline{U}_{CJ} + \epsilon S_0(\epsilon t)\cos(\alpha_i t) && (3.4)\\ \underline{l}^+ \cdot \underline{U}(z_3,t;\epsilon) &= \underline{l}^+ \cdot \underline{U}_{CJ} + \epsilon W_0(\epsilon t)\cos(\alpha_i t + \varphi)\,. && (3.5) \end{aligned}$$

Here $\underline{U}_{CJ}$ is the unperturbed burnt gas state, $\underline{l}^0$, $\underline{l}^+$ are the left eigenvectors of the matrix $\underline{\underline{A}}(\underline{U}_{CJ})$ associated with the eigenvalues $u_{CJ}$ and $(u+c)_{CJ}$ respectively and $\underline{\underline{A}}$ is the same as in (2.3) except that $\tilde{u}$ is replaced by $u = \tilde{u} + D_{CJ}$. (See Appendix A for more details.) Left-multiplication by $\underline{l}^0$, $\underline{l}^+$ filters out the entropy and backward acoustic contributions to the state vectors. Also in (3.4), (3.5) we allow for slow time variations of the amplitude functions $S_0$, $W_0$. This ansatz is justified in case that the linear growth rate, $\mathrm{Re}(\alpha)$, of the most unstable eigenmode is of order $O(\epsilon)$, i.e.,

$$\alpha = \epsilon\alpha_r^{(1)} + i\alpha_i\,, \quad \alpha_r^{(1)} = \vee(1) \quad (\epsilon \to 0)\,. \tag{3.6}$$

This relation specifies our notion of a marginal stability. At this stage the precise relations between $S_0$, $W_0$ and the phase shift $\varphi$ in (3.5) remain undetermined. For our model problem we let these quantities be constant and leave the derivation of equations for their long-time evolution for (Bdzil and Klein (1993)).

Closely following the procedure of Majda and Rosales (1984), we introduce a multiple scales perturbation ansatz:

$$\underline{U} = \underline{U}_{CJ} + \epsilon[V\underline{r}^- + S\underline{r}^0 + W\underline{r}^+] + \epsilon^2\underline{U}^{(2)}(x,t;\epsilon) \tag{3.7}$$

where the hyperbolic mode amplitudes depend on $(z,t;\epsilon z,\epsilon t)$, i.e.,

$$[V,S,W] = [V,S,W](z,t;\epsilon z,\epsilon t). \tag{3.8}$$

The right eigenvectors $\underline{r}^-, \underline{r}^0, \underline{r}^+$ of the matrix $\underline{\underline{A}}$ associated with the eigenvalues $u-c, u, u+c$, respectively, are given in Appendix A. At the leading order in $\epsilon$ one finds

$$\begin{aligned} V_t + (u-c)_{CJ} V_x &\equiv V_t = 0 \\ S_t + u_{CJ} S_x &= 0 \\ W_t + (u+c)_{CJ} W_x &= 0 . \end{aligned} \tag{3.9}$$

This gives rise to

$$\begin{aligned} V &= V(x; \epsilon z, \epsilon t) \\ S &= S(h; \epsilon z, \epsilon t) \\ W &= W(y; \epsilon z, \epsilon t) \end{aligned} \tag{3.10}$$

where the fast scale arguments are defined by

$$\begin{aligned} x &= z - (u-c)_{CJ} t \equiv z \\ y &= z - (u+c)_{CJ} t \\ h &= z - u_{CJ} t \equiv \tfrac{1}{2}(x+y) . \end{aligned} \tag{3.11}$$

They are characteristic coordinates for the forward and backward acoustic and the entropy mode, respectively.

At the second order one first derives equations analogous tc (3.9) for the mode amplitudes in $\underline{U}^{(2)}$, but with right hand sides depending on $V, S, W$ and their derivatives with respect to $(\epsilon z, \epsilon t)$. Then, by requiring $\underline{U}^{(2)}$ to be bounded even for $z, t = O(1/\epsilon)$, i.e., on the space-time scales for the action of weakly nonlinear effects, one obtains secular equations for the evolution of the first order mode amplitudes $V, S, W$ in the slow scale variables

$$\zeta = \epsilon z \qquad \text{and} \qquad \tau = \epsilon t . \tag{3.12}$$

These equations are

$$\begin{aligned} (V_\tau + (u-c)_{CJ} V_\zeta) - a[V - b\langle W \rangle + \langle S \rangle] V_x &= a \langle S W_y \rangle^{(x)} , \\ (S_\tau + u_{CJ} S_\zeta) + \langle W - V \rangle S_h &= 0 , \\ (W_\tau + (u+c)_{CJ} W_\zeta) - a[W - b\langle V \rangle + \langle S \rangle] W_y &= a \langle S V_x \rangle^{(y)} , \end{aligned} \tag{3.13}$$

where

$$\begin{aligned} a &= \tfrac{\gamma+1}{2} c_{CJ} \\ b &= \tfrac{3-\gamma}{\gamma+1} \end{aligned} \tag{3.14}$$

and $\langle \cdot \rangle$ and $\langle \cdot \rangle^{(x)}, \langle \cdot \rangle^{(y)}$ are fast variable averaging symbols. In particular, the superscripts $^{(x)}$ and $^{(y)}$ denote averaging at fixed $x$ and

$y$, respectively. The precise definitions of the averaging operations are given in Appendix B.

Next we introduce new slow time scale variables on the characteristic curves by

$$\begin{aligned} \eta &= a\left(\tau - \frac{\zeta}{(u+c)_{CJ}}\right), \\ \xi &= a\frac{\zeta}{2c_{CJ}}, \\ \vartheta &= \frac{\zeta}{u_{CJ}}. \end{aligned} \tag{3.15}$$

Then $\eta$ measures time along the forward acoustic characteristics $(z, \zeta = const)$, $\xi$ measures time after the passage through the lead shock along backward acoustic characteristics $(z-(u+c)_{CJ} = const)$, and $\vartheta$ measures time along the particle paths $(z - u_{CJ} = const)$. Using in addition the particle path label

$$\chi = \zeta - u_{CJ}\tau = \varepsilon h, \tag{3.16}$$

and reorganizing the slow scale dependencies of $V, S, W$ by

$$V = V(x;\xi,\eta), \qquad S = S(h;\chi,\vartheta), \qquad W = W(y;\xi,\eta), \tag{3.17}$$

we find

$$\begin{aligned} V_\eta - [V - b\langle W\rangle + \langle S\rangle]V_x &= -\langle SW_y\rangle^{(x)}, \\ S_\vartheta + \langle W - V\rangle S_h &= 0, \\ W_\xi + [W - b\langle V\rangle + \langle S\rangle]W_y &= \langle SV_x\rangle^{(y)}. \end{aligned} \tag{3.18}$$

Applying the fast variable averaging to these equations yields

$$\langle V\rangle_\eta = \langle S\rangle_\vartheta = \langle W\rangle_\xi \equiv 0 \tag{3.19}$$

so that

$$\langle V\rangle = \langle V\rangle(\xi), \qquad \langle S\rangle = \langle S\rangle(\chi), \qquad \langle W\rangle = \langle W\rangle(\eta) \tag{3.20}$$

and these functions are readily determined by the initial-boundary data. Requiring that there be no forward acoustic perturbation in the back of the wave at time $t = \tau = 0$, we have

$$\langle V\rangle \equiv 0. \tag{3.21}$$

Then, assuming for our model problem exact CJ conditions in the burnt gases we may set

$$\langle S\rangle(\chi) = \bar{S}(\chi) \equiv 0; \qquad \langle W\rangle(\eta) = \bar{W}(\eta) \equiv 0. \tag{3.22}$$

Notice that these conditions are assumed here, not derived. A complete second order analysis including the detonation reaction zone structure would yield long time evolution equations for the functions $S(\chi)$ and $W(\eta)$. It is in this sense that we are proposing a model problem here.

With (3.21), (3.22) the entropy equation in (3.16) decouples from the acoustic mode equations and we find

$$\begin{aligned} V_\eta - V V_x &= -(SW_y)^{(x)} \\ W_\xi + W W_y &= (SV_x)^{(y)} . \end{aligned} \tag{3.23}$$

The appropriate initial-boundary data for $V, W$ are

$$\begin{aligned} V(x;\xi,0) &= 0 \\ W(y;0,\eta) &= W_0 \cos(\alpha_r y) , \end{aligned} \tag{3.24}$$

and the entropy mode is explicitly given by

$$S(\frac{1}{2}(x+y);\lambda,\theta) = S_0 \cos(2\alpha_r \frac{x+y}{2} + \varphi) . \tag{3.25}$$

The system of equations (3.23) through (3.25) readily models the generation of forward acoustic perturbations in the burnt gases due to resonant energy transfer from the backward acoustic mode and we will describe a study of numerical solutions to these equations in (Bdzil and Klein (1991)). In the present paper we are mainly interested in the influence of these generated forward acoustics on the perturbations at the end of the reaction zone. From the discussion in the introduction we recall that this means to find the forward acoustic perturbations at a finite distance, $z_{1/N} = O(1)$ as $(\epsilon \to 0)$ behind the lead shock where $(1-\lambda) = 1/N$, $N$ fixed. In the current section the chemistry was completely negligible. To obtain the desired result on the influence of resonance effects at $x = z_{1/N}$, we have to match this burnt gas region to the main reaction zone, $(1-\lambda) = O(1)$. This matching procedure requires an analysis of two intermediate layers distinguished by different levels of chemical activity:
There is

i) a burnout layer, where $(1-\lambda) = O(\epsilon^2)$ and

ii) a transonic region, where $(1-\lambda) = O(\epsilon)$ as $(\epsilon \to 0)$.

We analyse the burnout layer in detail in section 4. This analysis will constitute our principal result that the resonance effects becomer weaker and weaker as one moves upstream towards the main reaction zone. A complete analysis of the matching through the transonic region is tedious but does not lead to new insights and thus we leave this discussion for a later more comprehensive report, (Bdzil and Klein (1993)).

## 4. The Burnout Layer

### 4.1 Asymptotic behavior of the reaction progress equation

In this subsection we are interested in a region behind the detonation structure where the effects of chemical heat release enter at the second order and therefore modify the acoustic resonances. To assess the extent of this region, we first consider the reaction progress equation $(2.1)_4$,

$$(1-\lambda)_t + u(1-\lambda)_z = -K(p,v)(1-\lambda). \tag{4.1}$$

The analysis will provide the correct scaling for the thickness of this asymptotic layer and will also yield the appropriate expansion scheme for the reaction progress variable, $\lambda$.

The general solution to (4.1) using the shock jump condition for the inert lead shock,

$$(1-\lambda) = 1 \qquad \text{at} \qquad z = 0 \tag{4.2}$$

reads

$$(1-\lambda) = \exp\left(-\overset{(m)}{\int_0^z} \frac{K(p,v)}{u}\, dz\right) \tag{4.3}$$

where the integration is along a particle path, $m = \text{const}$, with

$$\left.\frac{\partial t}{\partial z}\right|_m = \frac{1}{u(z,t)}. \tag{4.4}$$

With an asymptotic expansion of $K(p,v)$ and $u$ about the ZND profile according to

$$\begin{aligned} K(p,v) &= K(p^\circ,v^\circ) + \varepsilon\left((K_p)^\circ p^{(1)} + (K_v)^\circ v^{(1)}\right) + \dots \\ u &= u^\circ + \varepsilon u^{(1)} + \dots, \end{aligned} \tag{4.5}$$

the solution in (4.3) reads

$$(1-\lambda) = \exp\left(-{}^{(m)}\!\int_0^z \frac{K^*}{u^*}\,dz\right)\,\exp\left(-\varepsilon^{(m)}\!\int_0^z \left[\frac{K}{u}\right]^{(1)} dz\right) \quad \ldots\ (4.6)$$

where

$$\left[\frac{K}{u}\right]^{(1)} = \frac{1}{u^*}\Big[\quad (K_p)^* p^{(1)} + (K_v)^* v^{(1)} + (dK^*/dz)\,z^{(1)}\Big] - \frac{K^*}{(u^*)^2}\Big[u^{(1)} + (du^*/dz)z^{(1)}\Big] \qquad (4.7)$$

and $z^{(1)}$ is the first order perturbation of the particle path, $m$ = const. Obviously, (4.6) may be written as

$$(1-\lambda) = (1-\lambda)^*(1+O(\varepsilon)) \qquad (4.8)$$

and we conclude that in any region where $(1-\lambda) = O(\varepsilon^n)$ the proper expansion is

$$(1-\lambda) = \varepsilon^n \Lambda(z) + \varepsilon^{n+1}\lambda^{(n+1)}(z,t;\varepsilon z,\varepsilon t) + \ldots \qquad (4.9)$$

Furthermore, as $(1-\lambda)^* \to 0$, $K^* \to K_{CJ}, u^* \to u_{CJ}$ so that

$$\Lambda(z) = \exp(-\beta(z-z_n)) \qquad \text{with} \qquad \beta = \frac{K_{CJ}}{u_{CJ}} \qquad (4.10)$$

and with $z_n$ chosen so that $(1-\lambda^*)(z_n) = \varepsilon^n$. As a consequence, in the burnout layer we have

$$(1-\lambda) = \varepsilon^2 \exp(-\beta(z-z_2))\,(1+O(\varepsilon)) \qquad (4.11)$$

and the thickness of the layer is of order $\ln(1/\varepsilon)$. This result determines the appropriate choice of independent variables for the acoustic modes in this region as we will explain in the next subsection.

## 4.2 The influence of the reaction tail on the acoustic resonance

As for the burnt gas region we employ here a multiple scales expansion for the hyperbolic modes at first order. Before, we needed to introduce slow time varables, $(\eta,\xi,\vartheta)$ on each of the characteristics. In contrast, the residence time of entropy and backward acoustic perturbations in the burnout layer is of order $\ln(1/\varepsilon)$ only and this is insufficient to allow for accumulation of weakly nonlinear effects.

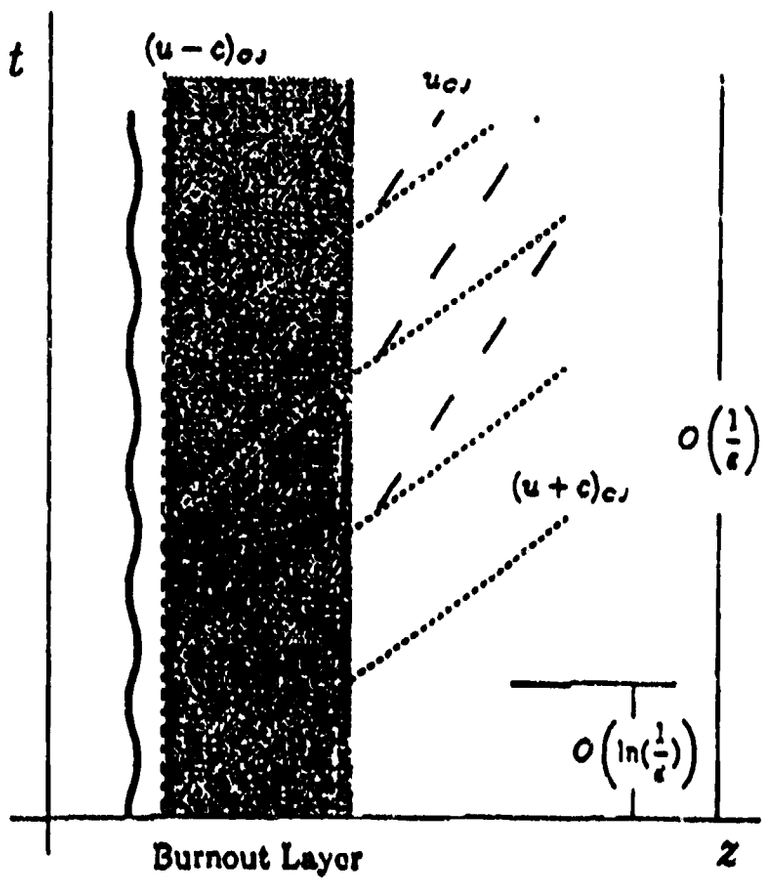


Fig. 4: Characteristics and their residence times in the burnout layer.

Only the forward acoustic characteristics have a long enough residence time in this layer as indicated in Fig. 4. The graph displays the forward and backward acoustic characteristics and particle paths and indicates the order of magnitude of the passage times of the respective characteristics through the burnout layer.

The appropriate expansion scheme in the present regime reads

$$\underline{U} = \underline{U}_{CJ} + \epsilon[\hat{V}\underline{r}^{-} + \hat{S}\underline{r}^{0} + \hat{W}\underline{r}^{+}] + \epsilon^{2}(\hat{\underline{U}}^{(2)}(z,t;\epsilon) + \Lambda(z)\underline{r}^{\lambda}) \quad (4.12)$$

where

$$\begin{aligned} \hat{V} &= \hat{V}(\hat{x};\eta) \\ \hat{S} &= \hat{S}(\tfrac{1}{2}(\hat{x}+y);\eta) \\ \hat{W} &= \hat{W}(y;\eta) \end{aligned} \quad (4.13)$$

and

$$\hat{x} = z - z_2 \quad (4.14)$$

with $z_2$ defined in (4.10), (4.11).

For our model problem we have assumed the backward traveling mode amplitudes $W_0, S_0$, the oscillation wave number, $\alpha_i$, and the phase shift, $\varphi$ in (3.4), (3.5) to be independent of the long time variable, $\eta$, and so we set explicitly

$$\begin{aligned} \hat{W} &\equiv W_0 \cos(\alpha_i y + \psi(\epsilon)) \\ \hat{S} &\equiv S_0 \cos(2\alpha_i \tfrac{(\hat{x}+y)}{2} + \varphi + \psi(\epsilon)). \end{aligned} \quad (4.15)$$

Here $\psi(\epsilon)$ is an $\epsilon$-dependent phase shift that makes the boundary data imposed on $S, W$ in the burnt gas region compatible with those for $\hat{S}, \hat{W}$ in the present regime.

The only secular constraint that remains is the long time evolution equation for $\hat{V}$, namely

$$\begin{aligned} \hat{V}_\eta - \hat{V}\hat{V}_{\hat{x}} &= \mu\Lambda(\hat{x}) + \langle \hat{S}\hat{W}_y \rangle^{(\hat{x})} \\ &= \mu \exp(-\beta\hat{x}) + \tfrac{1}{2}\alpha_i S_0 W_0 \sin(\alpha_i \hat{x} + \varphi + \psi). \end{aligned} \quad (4.16)$$

where $\mu = \ldots$ with $Q$ from (2.4). As initial condition we use the stationary unperturbed solution corresponding to the CJ-ZND profile, namely

$$\hat{V}(\hat{x},0) \equiv \hat{V}^{st}(\hat{x}) = \sqrt{\frac{2\mu}{\beta}} e^{-\frac{1}{2}\beta\hat{x}}. \quad (4.17)$$

This is the inviscid Burgers' equation driven by an explicit source term due to the combined effects of chemical heat release and weakly nonlinear acoustic resonance.

Notice that we merely need to solve these burnout layer equations in order to obtain the desired information on the influence of acoustic resonances on the perturbations in the upstream flow. There is an obvious physical interpretation of this formal result. On the time scales considered, $t = O(1/\epsilon)$, forward acoustic perturbations of order $O(\epsilon)$ can travel distances of no more than order $O(1)$ as $\epsilon \to 0$. The forward acoustics generated in the burnt gas region at distances $O(1/\epsilon)$ downstream from the detonation structure will thus not arrive in time to have any influence. The only perturbations that make it in time are those generated in the burnout layer. Since the generating backward traveling mode amplitudes, $\hat{W}, \hat{S}$, are given in this region directly by their upstream boundary data, (4.15), one only has to solve the single scalar equastion, (4.16), with inital data, (4.17), for the evolution of the forward acoustic mode amplitude.

A first straight-forward approach is via the method of characteristics. We construct this formal solution below and in particular derive the behavior of the solution as $\hat{x} \to -\infty$, which is needed for the upstream matching to the transonic region. Knowing that the characteristic solution is valid only as long as characteristic curves do not cross, i.e., for shock-free solutions, we present additional numerical solutions of (4.16), (4.17) in section 4.3. These solutions, in fact, reveal shock formation, but they verify the limit behavior of the solution for $\hat{x} \to -\infty$ as derived from the formal characteristic analysis.

Let $m = \text{const}$ denote a characteristic of (4.16), so that

$$\frac{\partial \eta}{\partial \hat{x}}\Big|_m = -\frac{1}{\hat{V}} \qquad \text{with} \qquad \eta(\hat{x}_0(m), m) = 0\,. \tag{4.18}$$

Without loss of generality we may choose $\hat{x}_0(m) = m$. Then (4.16) becomes

$$\frac{1}{2}\frac{\partial \hat{V}^2}{\partial \hat{x}}\Big|_m = -\mu \exp(-\beta \hat{x}) - \frac{1}{2}\alpha_i S_0 W_0 \sin(\alpha_i \hat{x} + \varphi + \psi)\,, \tag{4.19}$$

and the explicit solution in terms of $(\hat{x}, m)$ is

$$\hat{V}(\hat{x}, m) = \left\{ 2\frac{\mu}{\beta} e^{-\beta \hat{x}} + S_0 W_0 \left[ \cos(\alpha_i \hat{x} + \varphi + \psi) - \cos(\alpha_i m + \varphi + \psi) \right] \right\}^{1/2}. \tag{4.20}$$

To obtain the solution in terms of $(\hat{x}, \eta)$, one needs to construct the family of characteristic curves, $m = \text{const}$, by solving (4.18) numerically, using the solution in (4.20). The solution so constructed is

valid as long as neighboring characteristics do not cross. In that case, shock formation occurs and solution techniques capable of approximating weak solutions to nonlinear hyperbolic equations have to be employed as in section 4.3 below.

An expansion of (4.20) as $\hat{x} \to -\infty$ reads

$$\hat{V}(\hat{x},m) = \sqrt{\tfrac{2\mu}{\beta}}\left\{ e^{-\frac{\beta}{2}\hat{x}} \;-\; \tfrac{1}{4}e^{\frac{\beta}{2}\hat{x}}\tfrac{\beta}{4\mu}S_0W_0\left[\cos(\alpha_i\hat{x}+\varphi+\psi)-\cos(\alpha_i m+\varphi+\psi)\right]\right\}+\ldots \quad \text{as} \quad \hat{x}\to-\infty. \tag{4.21}$$

The terms in square brackets represent the influence of the initial data and of the acoustic resonance. These are multiplied by an exponential that decays as $\hat{x} \to -\infty$. In contrast, the first term, which corresponds to the background CJ-ZND solution diverges in this limit. For the matching to the upstream transonic layer we are interested in positions $\hat{x}$ where $(1-\lambda) = O(\varepsilon)$. According to (3.35), (3.38) this regime corresponds to

$$\hat{x} = \check{x} - \frac{1}{\beta}\ln(\frac{1}{\varepsilon}) \qquad \text{with} \qquad \check{x} = O(1) \qquad \text{as} \qquad (\varepsilon \to 0)\,. \tag{4.22}$$

Introducing (4.22) in (4.21) we find

$$\hat{V}(\hat{x},m) \;=\; \sqrt{\tfrac{2\mu}{\beta}}\left\{\varepsilon^{1/2}e^{-\frac{\beta}{2}\check{x}} \;-\; \varepsilon^{3/2}\tfrac{\beta}{4\mu}e^{\frac{\beta}{2}\check{x}}S_0W_0\left[\cos(\alpha_i\check{x}+\varphi+\check{\psi})-\cos(\alpha_i\check{m}+\varphi+\check{\psi})\right]\right\}+\ldots \quad \text{as} \quad \check{x}=O(1) \tag{4.23}$$

Here $\check{\psi}$ is a phase shift analogous to $\psi(\varepsilon)$ as explained below (4.15) and $\check{m}$ is defined in analogy with $\check{x}$ from (4.22). The immediate conclusions from the formula in (4.23) are that (i) the deviation of the solution from CJ-conditions is of order $O(\varepsilon^{1/2})$ now, but that (ii) the resonance effects no longer appear at order $O(\varepsilon)$ in the upstream transonic layer but at order $O(\varepsilon^{3/2})$ only.

The above derivations, based on the method of characteristics, are valid only as long as the solutions are shock-free and this is generally true only for some finite time. Therefore, in order to test the validity of the limit representation in (4.23) we present numerical solutions of the burnout layer problem, using modern higher order Godunov-type upwind techniques, in the next subsection.

A remark on the downstream matching of the burnout layer solution with the burnt gas region is in order. In the burnout layer solutions there is no degree of freedom in the backward traveling mode amplitudes, $\hat{S}, \hat{W}$, to accomodate the cumulative influence of the acoustic resonance. Thus, as $\hat{x} \to +\infty$, the second order perturbation, $\underline{U}^{(2)}$ diverges. This divergence, however, can be matched to the behavior of the backward traveling mode amplitudes, $S, W$ in the burnt gas region at $\xi = 0$, (Bdzil and Klein (1993)).

## 4.3 Numerical solutions of the burnout layer problem

Here we describe exemplary numerical solutions to equations (4.16), (4.17). We use a higher order MUSCL Godunov type upwind scheme, (see e.g. van Leer (1979) or LeVeq (1990)), to solve the homogeneous inviscid Burgers equation, $V_\eta - VV_x = 0$ and Strang-type operator splitting to account for the right hand side in (4.16). The sample results shown in Fig. 5 are based on the parameter set

$$\begin{aligned} W_0 &= S_0 = 1.0, \qquad \alpha_i = 2.0, \\ \mu &= 0.625, \qquad \beta = 0.2\,. \end{aligned} \tag{4.24}$$

Figure 5 shows a series of spatial distributions of the forward acoustic mode amplitude at different times, $\eta = 0.25, \eta = 1.5$. In both plots the solid line represents the initial data, which in turn coincide with the CJ-ZND background solution. As time evolves, the resonant source term generates oscillations around this background profile (Fig. 5a) and later on there is shock formation as seen in Fig. 5b. One common feature of both profiles is that the oscillations become weaker and weaker towards large negative $\hat{x}$. The deviations from the CJ-ZND background solution decay in this limit just as predicted by the limit analysis of the characteristic solution in section 4.2. To quantitatively verify the scalings implied by (4.21) we have computed the solution in the extended reion $-20 < \hat{x} < 30$. Figure 6a shows the distribution of $\hat{V}$ in $-20 < \hat{x} < 5$ at the time $\eta = 1.5$. Obviously the decay of the oscillations to the right as seen in Fig.5 continues. Figure 6 shows a scaled deviation from the CJ-ZND solution, $\hat{V}^{st}$, namely

$$V^* = (\hat{V} - \hat{V}^{st}) * [\hat{V}^{st}]^{1/2}\,, \tag{4.25}$$

as a function of $\hat{x}$ at the same time. According to (4.21) this quantity should be of order $O(1)$ as $\hat{x} \to -\infty$ and the plot verifies this

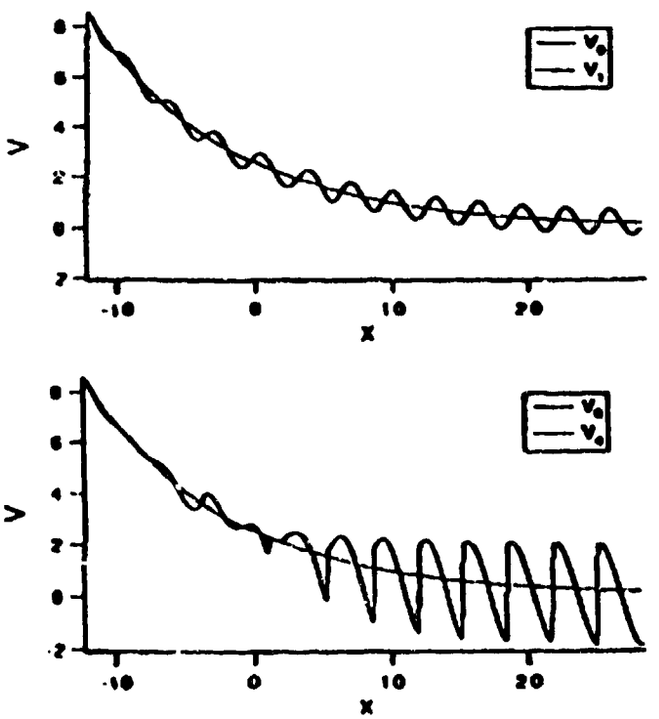


Fig. 5: Spatial profiles of the forward acoustic amplitude in the burnout layer at times: a) $\eta = 0.25$, b) $\eta = 1.5$.

tendency. In fact $V^*$ even seems to decay due to shock dissipation. Thus, for shock containing solutions the vanishing of the resonance effects in the upstream direction appears to be at least as pronounced as should be expected from the characteristic analysis.

## 5. Concluding Remarks

In this paper we have pointed out that for marginally stable near-Chapman-Jouguet detonations there is an apparent contradiction between *i)* the standard radiation boundary condition for linear stability analyses and *ii)* the resonant generation of forward acoustic perturbations in the back of the wave. We have identified a simplified asymptotic equation system that describes these weakly nonlinear resonance effects and we defined a model problem that will allow quantitative predictions and comparison with results from direct numerical simulations in future work.

It turned out that the proper formulation of farfield boundary conditions in a linear perturbation analysis of the detonation structure can be derived from solving a simplified system describing the resonance effects only in a so called burnout layer adjacent to the detonation structure. Formal solutions of the burnout layer equations based on the method of characteristics as well as numerical solutions of this burnout layer problem show that the influence of acoustic resonances decays as one leaves the burnout region upstream. A complete analysis, to be presented in Bdzil and Klein (1993), shows that this tendency continues and that at finite distances behind the lead shock of the detonation the acoustic resonance effects appear at no more than second order in the linear perturbation amplitude. We conclude that the standard radiation condition is valid even for near-CJ detonations.

## Appendix A: Eigenvalue Analysis

Eigenvalues:

$$a^- = u - c, \qquad a^0 = u, \qquad a^+ = u + c, \qquad a^{ch} = u, \qquad (A.1)$$

with $c = \sqrt{pv}$. Here $a^-, a^+$ are associated with acoustic wave propagation, $a^0$ with the advection of entropy perturbations and $a^{ch}$ with the advection of the chemical reaction progress variable. The asso-

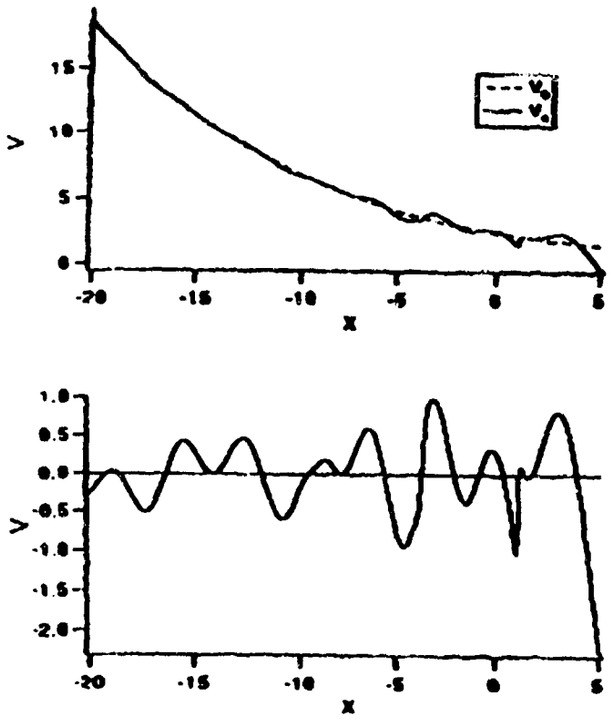


Fig. 6: a) Solution from Fig.5 at time $\eta = 1.5$ for large negative $\hat{x}$. b) Scaled deviation from the CJ-ZND background profile in the burnout layer according to (4.25), supporting the scaling behavior derived from a characteristic analysis as $\hat{x} \to -\infty$.

ciated right Eigenvectors are:

$$\underline{r}^{-} = \begin{pmatrix} -v \\ -c \\ \gamma p \\ 0 \end{pmatrix}, \ \underline{r}^{0} = \begin{pmatrix} v \\ 0 \\ 0 \\ 0 \end{pmatrix}, \ \underline{r}^{+} = \begin{pmatrix} -v \\ c \\ \gamma p \\ 0 \end{pmatrix}, \ \underline{r}^{ch} = \begin{pmatrix} 0 \\ 0 \\ 0 \\ 1 \end{pmatrix}. \quad (A.2)$$

and the left Eigenvectors are

$$\begin{array}{lllllll} l^{-} & = [ & 0, & -1/2c, & 1/2\gamma p, & 0, & ] \\ l^{0} & = [ & 1/v, & 0, & 1/\gamma p, & 0, & ] \\ l^{+} & = [ & 0, & 1/2c, & 1/2\gamma p, & 0, & ] \\ l^{ch} & = [ & 0, & 0, & 0, & 1, & ] \end{array} . \quad (A.3)$$

## Appendix B: Fast Variable Averaging Symbols

Let $s$ denote any of the fast variables, $x, y, h$ from (3.11) and let $\sigma = \varepsilon s$ be the related slow variable. Then the fast variable average of a multiple scales function $f(s, \sigma)$ is defined by

$$\langle f \rangle(\sigma) = \lim_{\Delta\sigma \to 0} \lim_{\varepsilon \to 0} \frac{\varepsilon}{2\Delta\sigma} \int_{\frac{1}{\varepsilon}(\sigma - \Delta\sigma)}^{\frac{1}{\varepsilon}(\sigma + \Delta\sigma)} f(s, \sigma)\, ds .$$

Notice the specific sequence of limits in this expression. Let further $g(x, y; \xi, \eta)$ with $\xi = \varepsilon x$, $\eta = \varepsilon y$, be some other multiple scales function depending on all of the slow and fast variables. Then

$$\langle g \rangle^{(x)}(x; \xi, \eta) = \lim_{\Delta\eta \to 0} \lim_{\varepsilon \to 0} \frac{\varepsilon}{2\Delta\eta} \int_{\frac{1}{\varepsilon}(\eta - \Delta\eta)}^{\frac{1}{\varepsilon}(\eta + \Delta\eta)} g(x, y; \xi, \eta)\, dy .$$

and an analogous definition holds for $\langle g \rangle^{(y)}(y; \xi, \eta)$.

## References


Bdzil J.B., Klein R., 1993. "Weakly Nonlinear Dynamics of Near-CJ Detonation Waves", in preparation.

Bourlioux A., Majda A.J., 1992. "Theoretical and Numerical Structure of Unstable Detonations", Prog. En. Comb. Sci, to appear.

Breitung W., 1991. "Conservative Estimates for Dynamic Containment Loads from Hydrogen Combustion", 11th Conference on Structural Mechanics in Reactor Technology, SMIRT, 11.

Erpenbeck J.J., 1962. "Stability of Steady State Equilibrium Detonations", Phys. Fluids, **5**, 604–614.

Erpenbeck J.J., 1963. "Structure and Stability of the Square Wave Detonation", in: 9th Symposium (Intl.) on Combustion, The Combustion Institute, Academic Press, **19**, 442–453.

Erpenbeck J.J., 1964. "Stability of Idealized One-Reaction Detonations", Phys. Fluids, **7**, 684–696.

Fickett W., Davis W.C., 1979. "Detonation", University of California Press, Berkeley.

Fujiwara T., Reddy K.V., 1989. "Propagation Mechanisms of Detonation – Three Dimensional Phenomena" in: Proc of 12th ICDERS, Ann Arbor, Michigan.

Lee H.I., Stewart D.S., 1990. "Calculation of Linear Detonation Instability: One-dimensional Instability of Plane Detonation", JFM, **216**, 103–132.

van Leer B., 1979. "Towards the Ultimate Conservative Difference Scheme V: A Second Order Sequel to Godunov's Method", J. Comp. Phys., **14**, 361–370.

LeVeq R.J., 1990. "Numerical Methods for Conservation Laws", Birkhäuser Verlag.

Majda A.J., Rosales R.R.,1984. Stud. Appl. Math., **71**, 149.

Majda A.J., Rosales R.R., Schönbeck M., 1988. "A canonical System of Integro-Differential Equations Arising in Resonant Nonlinear Acoustics", Stud. Appl. Math., **79**, 205–262.

Oran E.S., Boris J.P., 1987. "Numerical Simulation of Reactive Flow", Elsevier.

Shepherd J.E., 1985. "Chemical Kinetics of Hydrogen-Air-Diluent Detonations", in: Dynamics of Shock Waves, Explosions and Detonations, Eds.: J.R. Bowen, N. Manson, A K. Oppenheim, R.I. Soloukhin, 263–293.

Shepherd J.E., 1992. "Oblique Detonations and Propulsion", this volume.

Schoeffel S.U., 1992. "The Mechanism of Spinning Detonation - Numerical Study for Rectangular Crossection Tube", Proc. of 12th ICODERS; to be published.